

Controlled dynamics on energy landscapes

Karl Heinz Hoffmann^{1,a} and Johann Christian Schön²

¹ Institut für Physik, Technische Universität Chemnitz, 09107 Chemnitz, Germany

² Max-Planck-Institut für Festkörperforschung, Heisenbergstr. 1, 70569 Stuttgart, Germany

Received 14 November 2012 / Received in final form 25 January 2013

Published online 16 May 2013 – © EDP Sciences, Società Italiana di Fisica, Springer-Verlag 2013

Abstract. In systems with complex multi-minima energy landscapes, it is often not only the global minimum which is of great importance. For example, in materials science, metastable compounds corresponding to local minima on the landscape play a crucial role in many technological applications. In order to reach such modifications, both in computational and real world situations, it is necessary to optimally control the dynamics of the system on the landscape. We present a general method, how to design optimal temperature schedules for reaching particular basins on a complex landscape, by constructing a coarse-grained transition probability matrix from stochastic global landscape explorations, and subsequently using optimal control techniques on the Master equation describing the dynamics on the simplified energy landscape. As a demonstration example, the landscape of MgF_2 is considered.

1 Introduction

Trying to understand the dynamics of complex systems in science, technology and applied mathematics typically involves a detailed study of the energy or cost function landscape, which controls the time evolution of the system of interest [1]. Important quantities are the stable regions of the landscape [2–9] and the flow of probability as function of time [10,11], both as function of external environmental and control parameters. The former correspond to e.g. (meta)stable chemical compounds [6,7,12,13], folded or unfolded states of a protein [14–19], magnetic phases [20], stable attractors [21], or (sub)optimal solutions of combinatorial optimization problems [22,23], while the latter characterizes the likelihood of transitions between stable regions [24,25], the relaxation towards equilibrium [26,27], and the progress of optimization algorithms [23,28]. From a mathematical point of view, identifying such regions and flows involves the determination of the minima of the landscape and the local volume contained within the basins of the landscape, and the analysis of the connectivity of the landscape including the determination of the energetic, entropic and kinetic barriers [11,29] separating the minima and multi-minima basins [2].

Such a global exploration of the landscape using a large variety of methods and algorithms yields a detailed model that can explain many aspects of the dynamics of the underlying system, in particular the observed states, phases or chemical modifications, their individual stability and the transitions among them. However, in many instances, it proves to be quite difficult to actually access e.g. the global minimum or some particularly interesting metastable configuration of the system in practice,

even though our landscape information assures us of their potential existence. This is particularly noticeable in the fields of materials science and solid state chemistry, where the rational design of new compounds and routes for their synthesis has been lacking, and only in recent years a change from an inductive to a deductive approach to the field has been evolving [12,30]. Clearly, it would be of great interest, to develop a methodology that allows us to employ the available landscape information to design an optimal schedule of the available control parameters that drives the system of interest with a high probability to the desired region on the landscape.

Of course, this general issue has already been investigated in the past. Much work has been devoted to the development of optimal schedules for global optimization algorithms that purport to reach the global minimum of a given energy landscape in the most efficient fashion [23,31–34]. Similarly, one notes that the above problem can often be recast as a finite-time thermodynamics problem, where e.g. a particular thermodynamic state has to be reached within a finite time with a minimal use of resources [32,35]. Kunz et al. have used optimal control methods to analyze the dynamics on landscape models derived from clusters, with the goal to design an optimal simulated annealing schedule to reach a desired probability distribution in the configuration, for instance one focused at a particular structure in landscapes like a global minimum [36]. Their landscape model was based on information about the energies of the minima and the saddle points connecting them.

In this study, we solve a similar optimal control problem for a particular solid compound, MgF_2 , where the landscape model [24] is based on the energies of the minima, the local densities of states and the transition

^a e-mail: hoffmann@physik.tu-chemnitz.de

probabilities among the basins as function of energy, which have been measured using the so-called threshold algorithm [37,38]. We use this information to construct a transition probability matrix between the basins as function of temperature, employing so-called kinetic factors [11,29]. Thereafter we design optimal schedules that maximize the probability to reach a particular modification of MgF_2 . This system is of particular interest, since it is often compared with TiO_2 , for which several modifications such as rutile and anatase exist [39]; in contrast, however, MgF_2 has so far only been synthesized in the rutile [39] (and possibly a structurally closely related CaCl_2 [40]) modification, although the anatase modification occupies a large deep-lying basin on the energy landscape second in energy only to the rutile minimum [24].

2 The model system

2.1 Model description

The energy landscape of interest belongs to a simplified model of the solid compound MgF_2 that has been investigated in the past [41]. In that work, in order to reduce the number of degrees of freedom to a manageable size, MgF_2 was described by a periodically repeated variable unit cell containing two formula units of MgF_2 . No restrictions were placed on the possible movement of the atoms within the cell and neither on the changes of the unit cell parameters. Since many millions of energy calculations were needed to explore the energy landscape, the energy was computed using a simple Lennard-Jones-plus-Coulomb potential, where the magnesium and fluorine atoms were assigned charges +2 and -1, respectively, and the distance parameter in the Lennard-Jones potential was given by the sum of the ionic radii of the ions. For further details on the potential, we refer to reference [41].

In earlier work [24], the energy landscape of this model has been explored using the threshold algorithm [37,38], a stochastic walker-based exploration method, which explores the region of the landscape that is accessible from a given starting minimum without crossing a sequence of fixed energy lids. By sampling the distribution of states encountered during the free random walk below the lids, the local densities of states of the most important basins around the minima on the energy landscape were computed. Furthermore, by performing stochastic quenches along the trajectories, the transition probability among these basins as function of the energy level was measured. Note that these transition probabilities reflect both energetic, entropic and kinetic barriers separating the basins. Furthermore, if two minima were very closely related structurally and only separated by a very small energy barrier, they were assigned to the same minimum basin since the focus was on the large-scale structure of the landscape, not on the fine-tuning of structural distortions. Each such run was repeated several times, in order to improve the sampling statistics. From these data, a tree-graph representation of the landscape was

constructed [24], together with the so-called transition maps [24] and characteristic regions [42] of the landscape.

2.2 Data acquisition

Since the results of these threshold runs serve as the starting point of the analysis in this study, some more details regarding the data acquisition during these runs are presented below.

For the threshold-algorithm, the threshold (lid) set $\{E_\ell^{\text{th}}\}$ was used, in which the lids are spaced by 0.1 eV/atom and where the largest lid is E_1^{th} . For each lid and starting minimum, threshold runs of length up to 2.5×10^5 Monte-Carlo steps were performed, and every 5×10^4 steps, the random walker was quenched into the nearest local minimum. It was observed that the state space should be envisioned as a collection of minima with their respective basins, i.e. the set of states which under a quench leads to the minimum of the basin. These basins are weakly coupled at the energies of interest in the present study, i.e. inside such a basin local equilibrium can be established on a very short time scale compared to a typical transition time between the basins.

In particular, this separation of time scales argument allows us to visualize the probability flow among the minima, including their basins on the landscape, by writing the corresponding transition matrix as a product of three elementary probability matrices $\underline{\underline{Q}} \underline{\underline{H}} \underline{\underline{L}}$: the matrix $\underline{\underline{L}}$ describes the equilibration inside a given basin starting from its minimum, $\underline{\underline{H}}$ the horizontal flow of probability between neighboring basins at a given level of energy, and $\underline{\underline{Q}}$ the subsequent quench of all probability inside a given basin to its minimum. These matrices fulfill a dual purpose: they allow us to formally describe the action of the threshold algorithm on the level of transitions between basins and thus incorporate the data from the threshold runs. Secondly, these three matrices are sufficient to construct the transition matrices in the master equation that describes the probability flow among then minima at non-zero temperatures during the stochastic annealing procedure. In Section 3.2, we will give a more precise definition of the three matrices $\underline{\underline{Q}}$, $\underline{\underline{H}}$, and $\underline{\underline{L}}$.

The analysis of the threshold runs with their final quench yielded the transition frequencies $t_{j,k}(E_\ell^{\text{th}})$, which give the number of transitions from minimum k to minimum j for runs with threshold energy E_ℓ^{th} , and samplings of the numbers of states inside a basin $N_j(E_\ell^{\text{th}})$ below threshold energy E_ℓ^{th} [24,43]. For the transition frequencies, the observed numbers are small and thus one has to expect that they are susceptible to random fluctuations.

In order to obtain suitable input for our model, the data needs to be pre-processed. We note that within one basin the observed absolute number of states at a certain energy is not relevant in itself; it is only their ratio between energy levels which is important for the modelling [38]. Unfortunately we have no direct access to the ratio between the DOS of the different basins. Thus the

DOS is renormalized within a basin, i.e. the total number of states inside basin j is set to one,

$$d_j(E_\ell^{\text{th}}) = \frac{N_j(E_\ell^{\text{th}}) - N_j(E_{\ell+1}^{\text{th}})}{N_j(E_1^{\text{th}})}. \quad (1)$$

Here the data have been processed such that $d_j(E_\ell^{\text{th}})$ is the relative number (fraction) of states at energy E_ℓ^{th} .

As the number of runs starting from each single minimum are not necessarily equal, a renormalization of the transition frequencies is applied as well:

$$r_{j,k}(E_\ell^{\text{th}}) = t_{j,k}(E_\ell^{\text{th}}) / \sum_{j'} t_{j',k}(E_\ell^{\text{th}}). \quad (2)$$

Note that – contrary to the DOS – the rates $r_{j,k}(E_\ell^{\text{th}})$ describe the relative number of transitions below the threshold energy E_ℓ^{th} , not *at* energy E_ℓ^{th} . We stress already at this point that due to the underlying random walk properties the stationary distribution in state space should fulfill detailed balance. One of the consequences is that for each pair of basins a non-vanishing transition rate in one direction implies one in the opposite direction as well. Based on this data suitable typical data sets for systems with different numbers of basins were created in order to show different effects in this proof-of-concept paper.

3 The coarse-grained state space model

Based on these data sets, our aim is to construct a state space model of the system, which forms the basis for the dynamics we intend to describe. The dynamics will be developed in the form of a master equation, which allows not only to describe thermal relaxation at a fixed temperature, but which can also be used for analyzing the system's response to annealing schedules.

3.1 Model structure

The number of states in the state space of our system is too large by far to allow a direct modeling. Instead we coarse-grain the state space such that the model becomes treatable while yet preserving the dynamics. The weakly coupled basins in the energy landscape form the basis for this coarse-graining. Inside each basin the states are collected into a number of nodes at different energies. The set of states which are collected into a node are chosen such that they allow immediate equilibration on short time scales, i.e. one can assume local equilibrium in each node at any time. For the details of such an approach see references [26,44,45].

In our example system MgF_2 , the basins used correspond to the following six modifications (for structural data and explanation of the notation cf. Ref. [41]) which are abbreviated by the number in parenthesis: rutile (1), anatase (2), Mp1 (3), 1/2Ocp (4), CdI_2 (5), and 1/2BN (6).

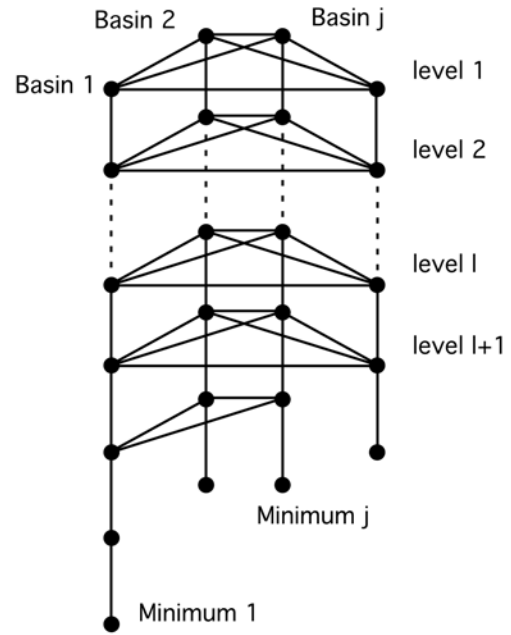


Fig. 1. The structure of the coarse-grained state space model. Note that the number of minima and their accompanying basins can vary. The nodes depict coarse-grained collections of states, and the lines show possible transitions between nodes. Each basin has its minimum at a certain level (and thus at a certain energy). The connections between a certain pair of basins has a minimum energy below which it is zero, i.e. no transition is possible.

We denote the nodes by a double index (j, i) , where j describes the basin and i the level of a node where the count starts at the top energy. For instance the DOS in basin j at level i is thus $d_{(j,i)} = d_j(E_i^{\text{th}})$. For an easy connection to the observed data the energies are chosen to be the set of $\{E_\ell^{\text{th}}\}$. The structure of the model is shown in Figure 1.

Based on the observed DOS we assign each basin its minimum at the lowest energy for which the DOS is different from zero. The corresponding level is denoted i_j^{min} . In Figure 1 the lines indicate possible transitions between nodes; however, only those between direct neighbors are shown. While inside each basin we assume that each node is connected to every other, transitions between basins are only possible between nodes at the same energy level.

The connections between a given pair of basins j and k have a minimum energy $E_{j,k}^G$ below which no transition is possible. This energy is obtained from the observed transition rates: the lowest energy for which either $r_{j,k}$ or $r_{k,j}$ is non-vanishing is chosen as $E_{j,k}^G$.

3.2 Incorporating the system data

As mentioned in Section 2.2, in order to build up the dynamics, it is convenient to introduce three transition probability matrices \underline{H} , $\underline{I}^{(\ell)}$, and \underline{Q} .

The matrix \underline{H} is a transition matrix which describes only *horizontal* transitions between the nodes of different

basins j and k at levels $i = n$, but not those inside a basin. This leads to a special structure of \underline{H} :

$$H_{(j,i),(k,n)} = \begin{cases} H_{j,k}^i & \text{if } j \neq k \text{ and } i = n, \\ 0 & \text{otherwise.} \end{cases} \quad (3)$$

The non-zero entries $H_{j,k}^i$ are as yet unknown, and it is one of the aims of this work to show how they can be determined.

The matrix $\underline{L}^{(\ell)}$ is a transition matrix which establishes local equilibrium inside each basin $j = k$ up to and including level ℓ in one step:

$$L_{(j,i),(k,n)}^\ell = \begin{cases} d_{(j,i)}^\ell & \text{if } j = k \text{ and } i_j^{\min} \leq \ell, \\ 0 & \text{otherwise,} \end{cases} \quad (4)$$

where

$$d_{(j,i)}^\ell = \frac{d_{(j,i)}}{D_j^\ell} \quad (5)$$

is a renormalized DOS. The renormalization is such that the DOS up to level ℓ add up to one:

$$D_j^\ell = \sum_{i=\ell}^{i_j^{\min}} d_{(j,i)}. \quad (6)$$

Note that the entries of $\underline{L}^{(\ell)}$ are taken from the observed density of states data and are thus known. Matrix $\underline{L}^{(\ell)}$ presupposes transitions between all nodes within one basin such that within one step local equilibrium in each basin is obtained.

Also needed is a quenching matrix \underline{Q} which represents the action of a thermal quench on the probability in the state space. In order to be compatible with the assumption that local equilibrium in each basin $j = k$ is established on the time scale of one step, \underline{Q} is chosen as

$$Q_{(j,i),(k,n)} = \begin{cases} 1 & \text{if } j = k \text{ and } i = i_j^{\min}, \\ 0 & \text{otherwise.} \end{cases} \quad (7)$$

Note that for both matrices, \underline{H} and \underline{Q} , the diagonal elements are reset such that the sums of the columns equal one:

$$H_{(j,i),(k,n)} = 1 - \sum_{j',i'} H_{(j',i'),(k,n)} \quad \text{if } (j,i) = (k,n), \quad (8)$$

$$Q_{(j,i),(k,n)} = 1 - \sum_{j',i'} Q_{(j',i'),(k,n)} \quad \text{if } (j,i) = (k,n). \quad (9)$$

Finally we need initial probability distributions that describe starting the dynamics in the minimum state of basin k

$$\hat{p}_{(j,i)}^k = \begin{cases} 1 & \text{if } j = k \text{ and } i = i_k^{\min}, \\ 0 & \text{otherwise.} \end{cases} \quad (10)$$

In terms of the quantities introduced above, we are now able to formulate the model equivalent to the observed

transition rates between basins $r_{j,k}(E_\ell^{\text{th}})$. First the system is prepared in one minimum, then – very rapidly compared to the typical transition times between basins – local equilibrium is established inside that basin. Thereafter the transitions between basins take place and finally a quench collects the probability in the minima of the basins:

$$r_{j,k}^{\text{mod}}(E_\ell^{\text{th}}) = \sum Q_{(j,i_j^{\min}),(j''',i''')} H_{(j''',i'''),(j'',i'')} L_{(j'',i''),(j',i')}^\ell \hat{p}_{(j',i')}^k, \quad (11)$$

or, in matrix notation

$$r_{j,k}^{\text{mod}}(E_\ell^{\text{th}}) = \left(\underline{Q} \cdot \underline{H} \cdot \underline{L}^\ell \cdot \underline{\hat{p}}^k \right)_{(j,i=i_j^{\min})}. \quad (12)$$

Inserting the above definitions of the quantities in (12) we obtain the simplified relation

$$r_{j,k}^{\text{mod}}(E_\ell^{\text{th}}) = \sum_{i'=\ell}^{i_k^{\min}} H_{j,k}^{i'} d_{(k,i')}^\ell. \quad (13)$$

The structure of the model was chosen such that in principle there is now enough data to determine all the $H_{j,k}^i$. However, if we were to replace $r_{j,k}^{\text{mod}}(E_\ell^{\text{th}})$ by $r_{j,k}(E_\ell^{\text{th}})$ and solve for the $H_{j,k}^i$ starting from the lowest level allowing transitions between any two basins, we would obtain transition rates which might not, and indeed do not, obey detailed balance. The reason for this are the fluctuations in the observed rates due to their small values, which can even lead to negative rates $H_{j,k}^i$ not allowed within the master equation dynamics.

But detailed balance is needed for a realistic consistent master equation dynamics, and we must therefore ensure that the transition rates and the densities of states fulfill this condition as closely as possible. Thus, in order to avoid these artifacts, we use a different approach instead. As a first step we determine the relative weights g_j of the DOS in each basin to combine them to the global DOS

$$d_{(k,n)}^{(\text{gl})} = d_{(k,n)} g_k. \quad (14)$$

As already stated above, we require that the horizontal transition matrix $H_{(j,i),(k,n)}$ is modelled such that detailed balance holds for the global DOS, i.e. $d_{(k,n)}^{(\text{gl})} = d_{(k,n)} g_k$ is the stationary distribution for $H_{(j,i),(k,n)}$. This implies for each triple (j, k, i) :

$$H_{j,k}^i d_{(k,i)}^{(\text{gl})} = H_{j,k}^i d_{(k,i)} g_k = H_{k,j}^i d_{(j,i)}^{(\text{gl})} = H_{k,j}^i d_{(j,i)} g_j. \quad (15)$$

Summing over all levels i energetically below or equal ℓ we obtain

$$\sum_{i=\ell}^{i_k^{\min}} H_{j,k}^i d_{(k,i)} g_k = \sum_{i=\ell}^{i_j^{\min}} H_{k,j}^i d_{(j,i)} g_j. \quad (16)$$

Starting from (13) and using (5) we find

$$r_{j,k}^{\text{mod}}(E_\ell^{\text{th}}) = \sum_{i=\ell}^{i_k^{\min}} H_{j,k}^i \frac{d_{(k,i)}}{D_k^\ell}. \quad (17)$$

Multiplication with D_k^ℓ results in

$$\sum_{i=\ell}^{i_k^{\min}} H_{j,k}^i d_{(k,i)} = r_{j,k}^{\text{mod}}(E_\ell^{\text{th}}) D_k^\ell, \quad (18)$$

which by inserting into (16) leads to

$$r_{j,k}^{\text{mod}}(E_\ell^{\text{th}}) D_k^\ell g_k = r_{k,j}^{\text{mod}}(E_\ell^{\text{th}}) D_j^\ell g_j. \quad (19)$$

While equation (19) holds for the model rates $r_{j,k}^{\text{mod}}(E_\ell^{\text{th}})$, this is not the case if we use the observed rates $r_{j,k}(E_\ell^{\text{th}})$ instead. In general

$$\epsilon_{j,k,\ell} = r_{k,j}(E_\ell^{\text{th}}) D_j^\ell g_j - r_{j,k}(E_\ell^{\text{th}}) D_k^\ell g_k \quad (20)$$

will not be zero. Of course, we want the deviation from detailed balance to be as small as possible, and thus we determine the g_j such that they minimize the deviation from the overall detailed balance requirement:

$$\begin{aligned} O_1 &= \sum_{j,k,\ell} w_{j,k,\ell} \epsilon_{j,k,\ell}^2 \\ &= \sum_{j,k,\ell} w_{j,k,\ell} (r_{k,j}(E_\ell^{\text{th}}) D_j^\ell g_j - r_{j,k}(E_\ell^{\text{th}}) D_k^\ell g_k)^2. \end{aligned} \quad (21)$$

Here $w_{j,k,\ell}$ are weights which can be adjusted to the different size of the density of states.

After the fractions g_j that characterize the contribution of the different basins to the global DOS have been determined, we turn to the still unknown horizontal transition probabilities $H_{j,k}^i$ of our model. Starting from the detailed balance requirement (15) for the $H_{j,k}^i$, we see that the ratio of the transition rates connecting two nodes is set by that requirement. We thus enforce this detailed balance requirement by setting

$$H_{j,k}^i = \frac{f_{\{j,k\}}^i}{d_{(k,i)} g_k}, \quad (22)$$

where $f_{\{j,k\}}^i \equiv f_{\{k,j\}}^i$ is the kinetic factor controlling the time scale of the transition rates between minima j and k at level i . From (18) we find

$$\begin{aligned} r_{j,k}^{\text{mod}}(E_\ell^{\text{th}}) D_k^\ell &= \sum_{i=\ell}^{i_k^{\min}} H_{j,k}^i d_{(k,i)} = \sum_{i=\ell}^{i_k^{\min}} \frac{f_{\{j,k\}}^i}{d_{(k,i)} g_k} d_{(k,i)} \\ &= \sum_{i=\ell}^{i_k^{\min}} \frac{f_{\{j,k\}}^i}{g_k}. \end{aligned} \quad (23)$$

While the above equation is valid for the model rates, it will not be so for the observed rates. Thus in general

$$\nu_{j,k,\ell} = r_{j,k}(E_\ell^{\text{th}}) D_k^\ell g_k - \sum_{i=\ell}^{i_k^{\min}} f_{\{j,k\}}^i \quad (24)$$

will not be zero.

Again we want the deviations from these conditions to be as small as possible, and thus for any pair $\{j,k\}$ we determine the $f_{\{j,k\}}^i$ such that they minimize the overall deviation:

$$O_{\{j,k\}} = \sum_{\ell} \nu_{j,k,\ell}^2 + \sum_{\ell} \nu_{k,j,\ell}^2. \quad (25)$$

Depending on the $r_{j,k}(E_\ell^{\text{th}})$, this procedure might lead for some states to overall transition rates which exceed one. In that case the kinetic factors are reduced at the respective level and are increased in the level which is energetically above to compensate for the change.

4 Optimal structure selection

4.1 Temperature-dependent transition rates

Based on the information obtained so far about the system, we can now study the relaxation of an arbitrary initial distribution over the minima and their basins. The dynamics is given by the master equation

$$P_{j,i}(t_{m+1}) = \sum_{k,n} G_{(j,i),(k,n)}(T(t_{m+1})) P_{(k,n)}(t_m), \quad (26)$$

in which the time increases in discrete steps from t_m to t_{m+1} . Here, the temperature dependent transition matrix $\underline{G}(T)$ is based on the matrix $\underline{L}^{(1)}$. While \underline{L} describes the transitions at infinite temperature, the finite temperature transition rates are obtained by a slight change: in order to establish local equilibrium at finite temperature, we introduce

$$L_{(j,i),(k,n)}(T) = \begin{cases} d_{(j,i)}(T) & \text{if } j = k \text{ and } i \leq i_j^{\min}, \\ 0 & \text{otherwise,} \end{cases} \quad (27)$$

where

$$d_{(j,i)}(T) = \frac{d_{(j,i)} e^{-\frac{E_j^{\text{th}}}{k_B T}}}{Z_j} \quad (28)$$

with

$$Z_j = \sum_i d_{(j,i)} e^{-\frac{E_j^{\text{th}}}{k_B T}} \quad (29)$$

is the local sum over states for basin j . Inserting the kinetic factors into the overall rates (22) we finally obtain $\underline{G}(T) = \underline{H} \underline{L}(T)$.

As in each basin local equilibrium is established before the transitions to the neighboring states take place, the overall transition probability from one basin to another one is not dependent on how the probability is distributed on the levels. Thus one can introduce coarse-grained transition probabilities between basins (which then become synonymous with their minima). In Figure 2 these transition probabilities are shown as a function of $x = \exp(-0.1/T)$, where the temperature is measured in units of the energy. In the remainder of this exposition, we will use x instead of T , but will still refer to it as ‘‘temperature’’. In order to stay consistent with the data available,

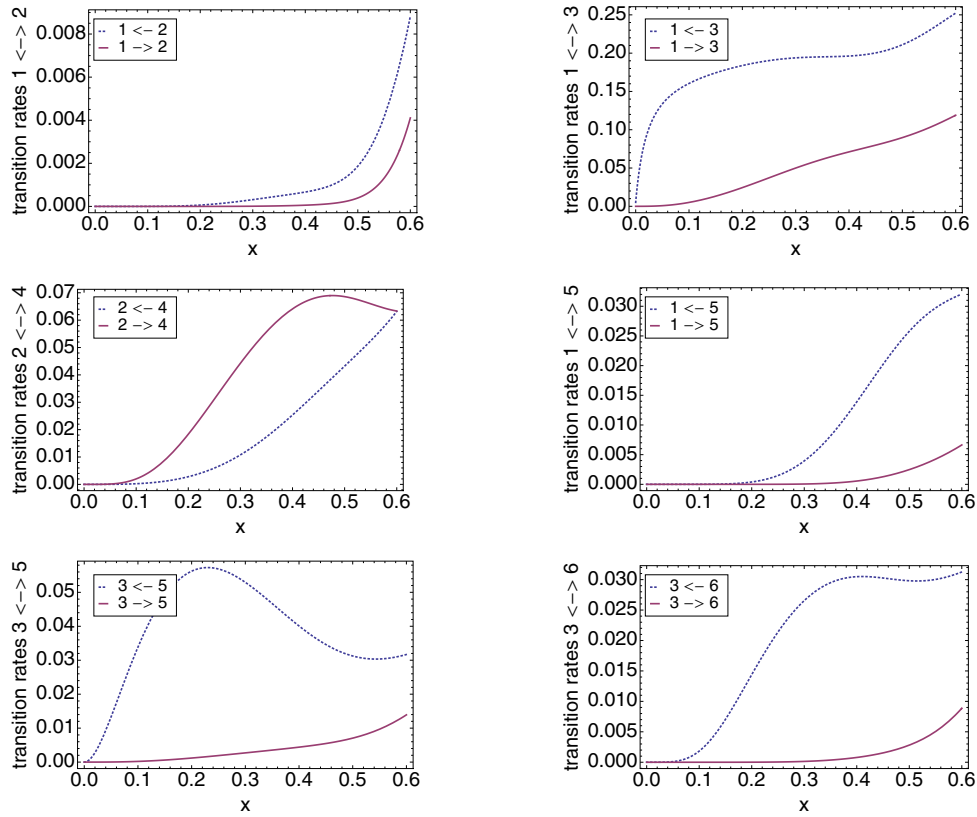


Fig. 2. The transition rates between different basins as obtained from the model are shown as a function of temperature. Here, the temperature was constrained to be within $0 \leq x \leq 0.6$, in order to ensure that the probability to be in a certain basin is only distributed over energies which had been explored during the data acquisition process. Note that there are large variations between forward and backward rates, which are in addition strongly temperature dependent. Thus they allow to control the dynamics in the state space by temperature changes.

we restrict the range of allowed x such that the probability is confined to energies below the maximum energy considered. Specifically, for all $x \leq 0.6$ the probability at the top level of the model is below 3%.

In the subplots of Figure 2, the transition probabilities between pairs of selected minima are shown. One sees that the transition probabilities are indeed temperature dependent. For the desired structure selection, it is important, of course, that the transition probabilities are of different magnitude at different temperatures, such that by varying the temperature, transitions from one minimum to another can be increased while others can be suppressed. For instance, at $x = 0.1$ the transitions from minimum 5 to 3 are elevated considerably, while 5 to 1 is more or less completely suppressed. Another example are the transition probabilities between 2 and 4, where for intermediate temperatures 2 to 4 dominates the back transition while at higher temperatures both transition probabilities are of the same size.

4.2 Optimizing the annealing schedule

The goal of our structure selection is to bring the system into one of its minima within a certain time horizon. Technically, the optimization is carried out by determining that

particular schedule which leads to the maximum probability to be in one of the minima within a given number of temperature steps.

The objective function Φ for this maximization is linear in the final probabilities:

$$\langle \Phi \rangle_M = \sum_j \Phi_j P_j(t_M), \quad (30)$$

where M is the number of steps available. To maximize the probability to be in minimum k , the objective Φ_j^k has to be chosen as

$$\Phi_j^k = \delta_{j,k}. \quad (31)$$

In all cases, the initial probability distribution $\hat{P}(t_0)$ was either taken to be uniform on the minima or a thermal equilibrium distribution at the maximum allowed temperature, i.e. at $x = 0.6$, was chosen.

Starting from $\hat{P}(t_0)$, we determine the final probability distribution $\underline{P}(t_M)$ from the master equation (26). The optimal schedule $T_{\text{opt}}(t_m)$ is then computed by an iterative algorithm based on control theory; for details see [46–48]. The algorithm proceeds by successive modifications of an initial annealing schedule. For each schedule the probability distribution at every time step is calculated starting from an initial distribution. Basically, $\langle \Phi \rangle_M$ has to

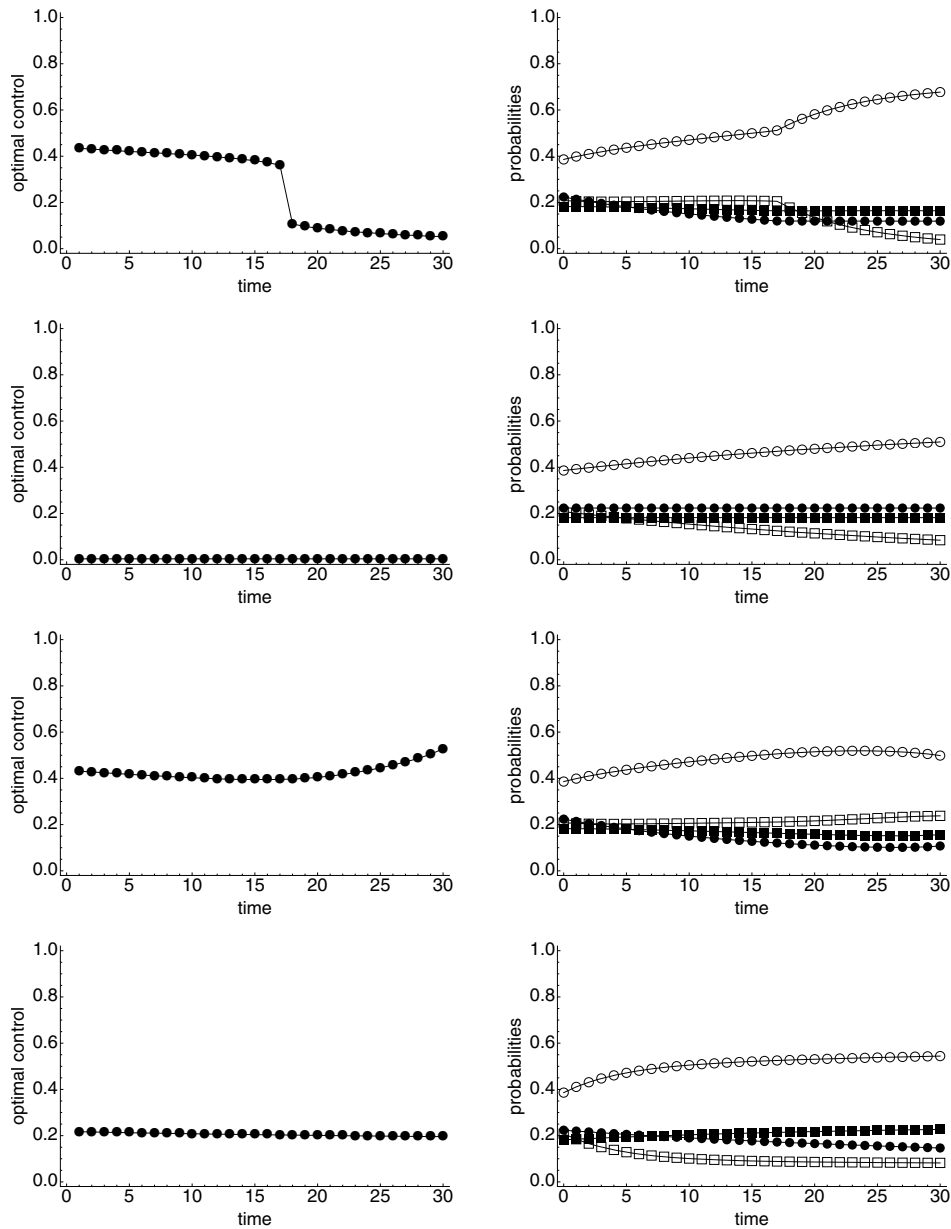


Fig. 3. Starting from a T_{\max} -distribution on the left from top to bottom the optimal temperature schedules to maximize the likelihood to be in basins rutile (1), anatase (2), Mp1 (3), and 1/2Occp (4), respectively, are shown. On the right the corresponding time evolution of the probability distributions are shown: rutile (1, open circle), anatase (2, filled circle), Mp1 (3, open square), and 1/2Occp (4, filled square).

be maximized as a function of the variables $T(t_m)$, where $\langle \Phi \rangle_M$ depends on the $T(t_m)$ through the final distribution $\underline{P}(t_M)$. This maximization is constrained by equation (26). Introducing Lagrange parameters $\underline{\Delta}^{\text{tr}}(t_m)$ the functional

$$F = \langle \Phi \rangle_M + \sum_{m=0}^{M-1} \underline{\Delta}^{\text{tr}}(t_{m+1}) (\underline{G}(T(t_{m+1})) \underline{P}(t_m) - \underline{P}(t_{m+1})) \quad (32)$$

is maximized using the usual optimal control principles. The number of iterations needed for the algorithm to converge is rather small, on the order of ten.

4.3 Results

In this subsection, we consider a reduced system by taking only the four basins with the lowest energy, i.e. rutile (1), anatase (2), Mp1 (3), and 1/2Occp (4), into account.

For each of these basins we determined optimal annealing schedules for the two different starting distributions discussed above. The number of available steps M was chosen to be 15 and 30. The schedules for the T_{\max} -distribution and the uniform distribution are shown in Figures 3 and 4, respectively.

The figures show on the left from top to bottom the optimal schedule to maximize the probability to be in basin

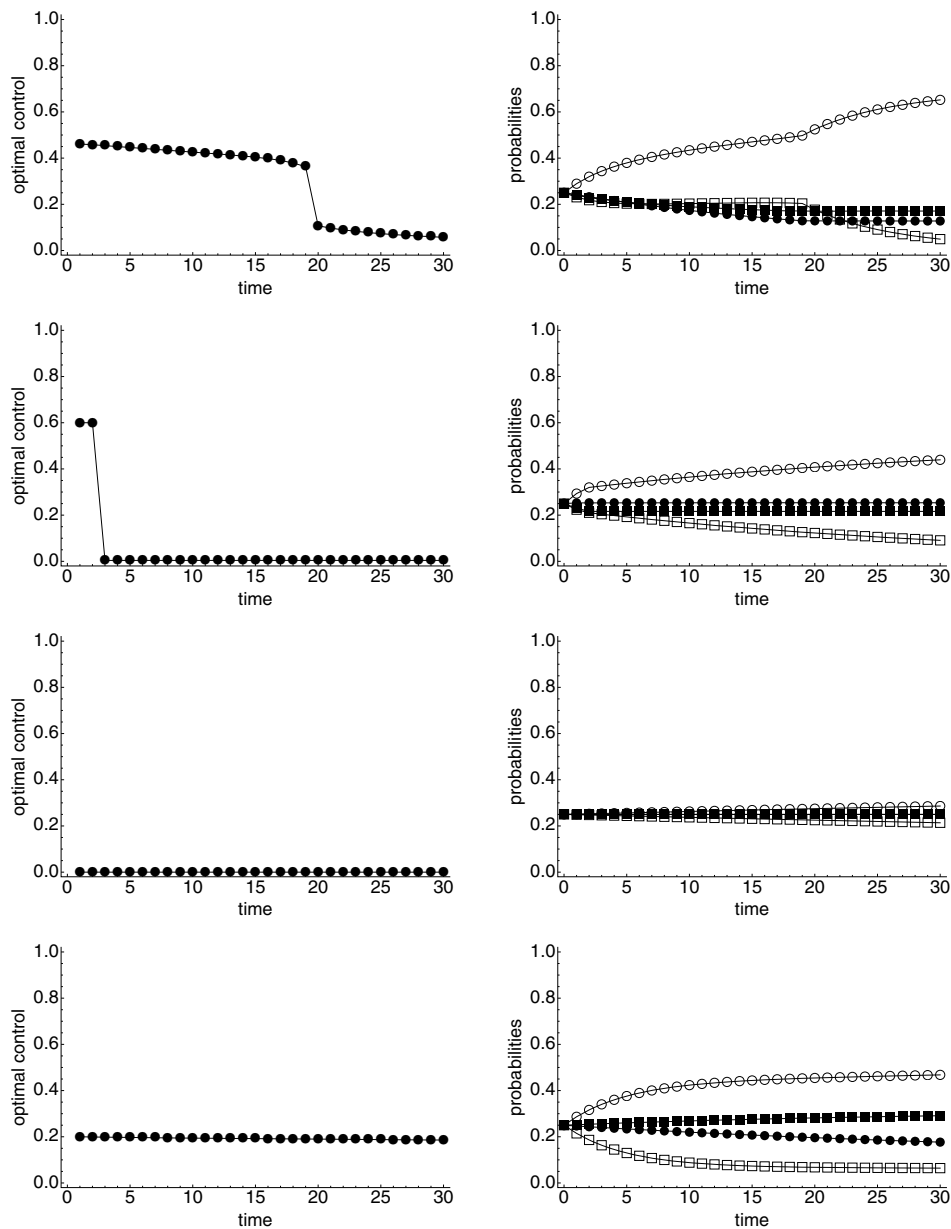


Fig. 4. Starting from a uniform distribution on the left from top to bottom the optimal temperature schedules to maximize the likelihood to be in basins rutile (1), anatase (2), Mp1 (3), and 1/2Occp (4), respectively, are shown. On the right the corresponding time evolution of the probability distributions are shown: rutile (1, open circle), anatase (2, filled circle), Mp1 (3, open square), and 1/2Occp (4, filled square).

rutile (1), anatase (2), Mp1 (3), and 1/2Occp (4), respectively. The control shown is $x = \exp -0.1/T$, where T is measured in units of the energy (eV/atom). On the right the corresponding time evolution of the probability distributions are shown: rutile (1, open circle), anatase (2, filled circle), Mp1 (3, open square), and 1/2Occp (4, filled square).

In both figures one can see a number of interesting effects and partly unexpected features.

Let us first look at Figure 3 displaying the data for starting with a T_{\max} -distribution. First of all we see that the optimal schedules are different for the respective minima. While anatase requires a quench, i.e. zero

temperature annealing, to collect as much probability as possible, 1/2Occp, a rather high lying minimum, needs an intermediate schedule of low moderate temperatures. Mp1 needs a schedule at intermediate temperatures, which rises at the end of the schedule towards the maximum allowed temperature.

The most surprising is the schedule for rutile. Here we start with slightly falling intermediate temperatures, which at step 18 are suddenly reduced to less than half of the temperature. The effect is clearly seen in the probability distribution: while the target probability to be in the rutile basin first increases at a moderate rate, at step 18 the increase is jumping up. The probability is drained

Table 1. The final population probabilities for the basins after optimal annealing with $M = 15$ and $M = 30$ steps, starting from a uniform distribution. For $M = 0$ the initial distribution is shown.

M	Rutile	Anatase	Mp1	0.5Occp
0	0.25	0.25	0.25	0.25
15	0.539979	0.253529	0.231165	0.276389
30	0.652078	0.253529	0.213749	0.291088

from the anatase basin, while the probabilities in Mp1 and 1/2Occp seem to be more or less unaffected. We note that this might be related to the different trapping temperatures $T_{\text{trap}}(1)$ and $T_{\text{trap}}(2)$ of the rutile and anatase basins, respectively, [24] in the energy region of the landscape where the transition between these two basins takes place: since $T_{\text{trap}}(2) < T_{\text{trap}}(1)$, we expect to observe a flow of probability from the anatase basin to the rutile basin for in-between temperatures, $T_{\text{trap}}(2) < T < T_{\text{trap}}(1)$.

Similar results can be seen in Figure 4. Again the schedule for maximizing the probability to be in the rutile basin shows the jump with equivalent results, and the schedule for anatase remains nearly unchanged. Very different is the schedule to maximize the chance to find the Mp1 configuration: now a $T = 0$ schedule is required. Nonetheless, the Mp1 probability decays during the time evolution. An explanation for that behavior will follow below. The 1/2Occp schedule remains more or less unchanged. This is certainly partly explained by the fact that for both starting distributions the 1/2Occp-values are not too far apart.

From the probabilities in Table 1 one can see that for rutile, anatase, and 1/2Occp the optimal annealing leads to an increase in the final probabilities, while Mp1 is losing against its initial start value of 0.25. That seems astonishing as Mp1 has its minimum at an energy lower than 1/2Occp. But on closer inspection one sees that Mp1 has non-vanishing transitions into rutile at the energy of its minimum, which makes it unstable within our model even at zero temperature. The reason for this is the tiny energy barrier separating the Mp1 and the rutile basins [24], which during the model construction described here (based on energy levels spaced by 0.1 eV) results in a non-zero transition probability already in the first discrete energy level bin. Thus starting from a uniform distribution, the best a zero temperature schedule can do is to slow down the decay of the probability to be in Mp1.

When starting from the T_{max} -distribution, the results are different: here, a schedule as shown can even increase the probability to be in the Mp1 configuration as can be seen from Table 2.

5 Discussion and summary

In this study, we addressed the problem whether it is possible to increase the yield of a specified configuration of a chemical compound by controlling the dynamics on the

Table 2. The final population probabilities for the basins after optimal annealing with $M = 15$ and $M = 30$ steps, starting from a distribution at maximum temperature. For $M = 0$ the initial distribution is shown.

M	Rutile	Anatase	Mp1	0.5Occp
0	0.386089	0.22364	0.208031	0.18224
15	0.58667	0.22364	0.225918	0.212332
30	0.677186	0.22364	0.237732	0.227075

energy landscape of the system. We presented a road map to achieve that goal, using a particular solid compound, MgF_2 , as an example. In a first step, a coarse-grained landscape model based on the energies of the minima, the local densities of states and the transition probabilities among the basins as function of energy is developed. The data needed for this model is extracted from the results of dynamical test runs performed by the so-called threshold algorithm, which explores the regions of the landscape that are accessible from a given set of starting minima without crossing a sequence of fixed energy lids. Next, we use this information to construct a transition probability matrix as function of temperature, which reflects the energetic, entropic and kinetic barriers separating the basins, and allows a complete description of the dynamics on the coarse-grained model of the energy landscape. Finally, we use standard optimal control procedures to design optimal schedules that maximize the probability to reach a particular basin on the landscape for a given initial probability distribution on the various minima of the landscape.

In the example system, this translated into finding the temperature schedule for which the system has the highest likelihood to reach a specified modification of MgF_2 . For each of the possible modifications we determined optimal annealing schedules for two different starting distributions on the minima: a uniform distribution, where the probability to be in a basin initially was 0.25, and the thermal equilibrium distribution at the highest allowed temperature. For concreteness, the number of available temperature steps M was chosen to be 15 and 30. By this approach we were able to show that the control of annealing procedures can significantly increase the probability to be in certain regions of the state space of MgF_2 . For example, the final occupation probability for the energetically high-lying minimum structure 1/2Occp can be increased by more than 20% compared to a uniform starting distribution or the thermally equilibrated distribution, and similarly the probability to reach the global minimum rutile already within the very short finite time available can be more than doubled.

Of course, for technical reasons, the example landscape chosen was highly simplified compared to the much more complex landscape of real MgF_2 . Nevertheless, it reflects many of the qualitative if not quantitative features of the real system, and the procedure we have presented can be transferred essentially one-to-one to more complex systems and applications. Thus, one would expect that by combining optimal control methods with information

gained from global landscape explorations, both on the theoretical and experimental side, it will be possible to design temperature schedules that will assist the experimental solid state chemist and physicist in improving the yield of their syntheses of particular modifications of solid compounds [49,50]. Besides applying our approach to the study of more complex landscapes, further research will be directed towards a deeper understanding of the intricate relation of the temperature dependent transition rates between basins. In this context, it seems worthwhile to study and improve the data acquisition procedures to save on the computational investment needed for constructing the coarse-grained transition probability matrix. Here, one possible extension may be to use the ParQ-methods [51] that should allow for a more efficient scanning of the landscape.

References

- D.J. Wales, *Energy Landscapes with Applications to Clusters, Biomolecules and Glasses* (Cambridge University Press, Cambridge, 2004)
- J.C. Schön, M. Jansen, *Int. J. Mat. Res.* **100**, 135 (2009)
- S.H. Northrup, J.T. Hynes, *J. Chem. Phys.* **73**, 2700 (1980)
- R.F. Grote, J.T. Hynes, *J. Chem. Phys.* **73**, 2715 (1980)
- H. Grubmüller, *Phys. Rev. E* **52**, 2893 (1995)
- J.C. Schön, M. Jansen, *Z. Kristallogr.* **216**, 307 (2001)
- J.C. Schön, M. Jansen, *Z. Kristallogr.* **216**, 361 (2001)
- J.-P. Aubin, A. Lesne, *J. Math. Phys.* **46**, 043508 (2005)
- S.R. Williams, D.J. Evans, *J. Chem. Phys.* **127**, 184101 (2007)
- J.C. Schön, M.A.C. Wevers, M. Jansen, *J. Phys.: Condens. Matter* **15**, 5479 (2003)
- K.H. Hoffmann, J.C. Schön, *Found. Phys. Lett.* **18**, 171 (2005)
- J.C. Schön, M. Jansen, *Angew. Chem. Int. Ed.* **35**, 1286 (1996)
- S.M. Woodley, R. Catlow, *Nat. Mater.* **7**, 937 (2007)
- A.-C. Garcia, in *Proceedings of Les Houches School on Nonlinear Excitations in Biomolecules, Les Houches, 1994*, edited by M. Peyrard (Springer, Berlin, 1994), pp. 191–208
- S. Govindarajan, R.A. Goldstein, *Proteins: Struct. Funct. Gen.* **29**, 461 (1997)
- S. Govindarajan, R.A. Goldstein, *Biopolymers* **42**, 427 (1997)
- S.V. Krivov, M. Karplus, *Proc. Natl. Acad. Sci.* **101**, 14766 (2004)
- Y. Fukunishi, *Proteins: Struct. Funct. Gen.* **33**, 408 (1998)
- H. Frauenfelder, P.W. Fenimore, R.D. Young, *IUBMB Life* **59**, 506 (2007)
- P. Sibani, *Physica A* **258**, 249 (1998)
- T. Komatsuzaki, K. Hoshino, Y. Matsunaga, *Regularity in Chaotic Transitions on Multibasin Landscapes*, in *Advances in Chemical Physics, Part B*, edited by M. Toda, T. Komatsuzaki, T. Konishi, R. Stephen Berry, S.A. Rice (Applications to Chemical Reaction Dynamics in Complex Systems, Wiley, New York, 2005), Vol. 130, pp. 257–313
- P. Sibani, J.C. Schön, P. Salamon, J.O. Andersson, *Europhys. Lett.* **22**, 479 (1993)
- P. Salamon, P. Sibani, R. Frost, *Facts, Conjectures, and Improvements for Simulated Annealing*, in *Monographs on Mathematical Modeling and Computation*, 1st edn. (SIAM, Philadelphia, 2002), Vol. 7
- M.A.C. Wevers, J.C. Schön, M. Jansen, *J. Phys.: Condens. Matter* **11**, 6487 (1999)
- C.-B. Li, Y. Matsunaga, M. Toda, T. Komatsuzaki, *J. Chem. Phys.* **123**, 184301 (2005)
- K.H. Hoffmann, P. Sibani, *Phys. Rev. A* **38**, 4261 (1988)
- P. Sibani, K.H. Hoffmann, *Phys. Rev. Lett.* **63**, 2853 (1989)
- C. de Groot, D. Würtz, K.H. Hoffmann, in *Parallel Problem Solving from Nature*, edited by H.P. Schwefel, R. Maenner (Springer-Verlag, Berlin, 1991), pp. 445–454
- A. Fischer, K.H. Hoffmann, J.C. Schön, *J. Phys. A* **44**, 1 (2011)
- M. Jansen, J.C. Schön, *Angew. Chem. Int. Ed.* **45**, 3406 (2006)
- B. Andresen, K.H. Hoffmann, K. Mosegaard, J. Nulton, J.M. Pedersen, P. Salamon, *J. Phys.* **49**, 1485 (1988)
- P. Salamon, J.D. Nulton, J.R. Harland, J. Pedersen, G. Ruppeiner, L. Liao, *Comput. Phys. Commun.* **49**, 423 (1988)
- K.H. Hoffmann, D. Würtz, C. de Groot, M. Hanf, *Concepts in Optimizing Simulated Annealing Schedules: an Adaptive Approach for Parallel and Vector Machines*, in *Parallel and Distributed Optimization*, edited by M. Grauer, D.B. Pressmar (Springer-Verlag, Berlin, Heidelberg, New York, 1991), pp. 154–175
- J. Lässig, K.H. Hoffmann, *Phys. Rev. E* **79**, 046702 (2009)
- Finite-Time Thermodynamics and Thermoeconomics*, edited by S. Sieniutycz, P. Salamon (Taylor and Francis, New York, 1990)
- R.E. Kunz, P. Blaudeck, K.H. Hoffmann, R.S. Berry, *J. Chem. Phys.* **108**, 2576 (1998)
- J.C. Schön, *Ber. Bunsenges.* **100**, 1388 (1996)
- J.C. Schön, H. Putz, M. Jansen, *J. Phys.: Condens. Matter* **8**, 143 (1996)
- A.R. West, *Solid State Chemistry and Its Applications* (Wiley, New York, 1984)
- A. Bach, D. Fischer, X. Mu, W. Sigle, P.A. van Aken, M. Jansen, *Inorg. Chem.* **50**, 1563 (2011)
- M.A.C. Wevers, J.C. Schön, M. Jansen, *J. Solid State Chem.* **136**, 223 (1998)
- M.A.C. Wevers, J.C. Schön, M. Jansen, *J. Phys. A* **34**, 4041 (2001)
- M.A.C. Wevers, *Energetische und entropische Aspekte der Energielandschaften von MgF_2 , CaF_2 und $Li_xNa_{6-x}N_2$ ($x = 0, 1, \dots, 6$) sowie ein Vergleich mit ab-initio-Rechnungen*, Ph.D. thesis, University of Bonn, 1999
- K.H. Hoffmann, P. Salamon, *Appl. Math. Lett.* **22**, 1471 (2009)
- K.H. Hoffmann, P. Salamon, *Physica A* **390**, 3086 (2011)
- V.F. Krotov, *Control and Cybernetics* **17**, 115 (1988)
- K. Ergenzinger, K.H. Hoffmann, P. Salamon, *J. Appl. Phys.* **77**, 5501 (1995)
- A. Franz, K.H. Hoffmann, *J. Comput. Phys.* **176**, 196 (2002)
- M. Santoro, J.C. Schön, M. Jansen, *Phys. Rev. E* **76**, 1 (2007)
- J.C. Schön, *Z. Anorg. Allg. Chem.* **635**, 1794 (2009)
- F. Heilmann, K.H. Hoffmann, *Europhys. Lett.* **70**, 155 (2005)